Stem Cell Research 17 (2016) 607–615

Contents lists available at ScienceDirect

Stem Cell Research

journal homepage: www.elsevier.com/locate/scr

Immune cell recruitment in teratomas is impaired by increased Wnt secretion

Iris Augustin [a,*], Dyah L. Dewi [a], Jennifer Hundshammer [a], Eugen Rempel [a], Fabian Brunk [b], Michael Boutros [a]

[a] German Cancer Research Center (DKFZ), Div. of Signaling and Functional Genomics, and Heidelberg University, Department of Cell and Molecular Biology, Medical Faculty Mannheim, Heidelberg University, Heidelberg 69120, Germany
[b] German Cancer Research Center (DKFZ), Div. of Developmental Immunology, Heidelberg 69120, Germany

ARTICLE INFO

Article history:
Received 31 October 2015
Received in revised form 16 October 2016
Accepted 25 October 2016
Available online 29 October 2016

Keywords:
Wnt signaling
Embryonic stem cells
Teratoma
Immune surveillance

ABSTRACT

Wnt signaling plays a central role in tumor initiation and tumor progression. Mutations in Wnt pathway components, such as the tumor suppressor APC, lead to malignant transformation. While previous studies focused on Wnt-related changes in cancer cells, the impact of aberrant Wnt signaling on the tumor microenvironment is only beginning to emerge. In order to investigate the role of increased Wnt secretion on tumor growth and the microenvironment, we generated a novel germ cell tumor model by overexpressing the Wnt secretion factor Evi/Wls in mouse embryonic stem cells. Evi-overexpressing teratoma were characterized by enhanced tumor growth in supporting a tumor-promoting role of Wnt secretion. Interestingly, enhanced Evi expression correlated with impaired immune cell recruitment. Specifically, T- and B-cell infiltration was reduced in Evi-overexpressing teratomas, which was independent of teratoma size and differentiation. Our study suggests that Wnt secretion impairs immunosurveillance. Since immune cell infiltration has been shown to have prognostic value, the levels of secreted Wnt activity might impact the efficiency of cancer immunotherapy.

1. Introduction

Cells of the tumor microenvironment exert context-dependent pro- and anti-tumorigenic functions (de Visser et al., 2006; Hanahan and Weinberg, 2011). Tumor-infiltrating leukocytes execute critical functions within the complex interactions of tumor cells with their microenvironment. Immunosurveillance mechanisms within the tumor stroma enable the immune system to recognize transformed cells in order to initiate mechanisms of their inhibition or elimination (Dunn et al., 2002; Dunn et al., 2004; Schreiber et al., 2011). During immunosurveillance, cells of the innate and the adaptive immune system cooperate to prevent the growth of neoplastic tissues (Mittal et al., 2014). The cascade starts with an inflammatory signal produced by the tumor cells, which leads to the recruitment of natural killer (NK) cells, macrophages and dendritic cells (DC), followed by T-cell infiltration and activation of their cytotoxic function.

Recent meta-analyses of solid tumors have shown that the $CD3^+$ T cells infiltration correlates with good prognosis (Gooden et al., 2011; Hwang et al., 2012; Mittal et al., 2014; Nakano et al., 2001; Sato et al., 2005; Sharma et al., 2007). However, it is an open question why some tumors are highly infiltrated by T cells and others are not. Recent reports suggest that Wnt/β-catenin signaling in melanoma impairs the antitumor immune response and thereby supports cancer cell-induced immunosuppression (Spranger et al., 2015; Yaguchi et al., 2012). Thus, the better understanding of the involved signaling mechanisms may provide insights into the immune escape mechanisms of tumor cells.

The highly conserved transmembrane molecule Evi/Wls/Gpr177 is an essential component of the Wnt secretion machinery (Banziger et al., 2006; Bartscherer et al., 2006). It is required for the exocytosis of Wnt proteins acting as a Wnt cargo receptor by shuttling between the Golgi, the plasma membrane and endosomal compartments (Bartscherer and Boutros, 2008). Evi is a single-gene family in vertebrates (Jin et al., 2010; Port and Basler, 2010). Thus, it has been assumed that Evi is involved in the secretion of all Wnt proteins. Correspondingly, Evi depletion globally affects Wnt signaling with consequences for canonical as well as non-canonical Wnt signaling. This, in turn, can be exploited as a unique experimental tool to modulate Wnt signaling through the regulation of Wnt ligand secretion. Genetic inactivation of Evi in mice results in embryonic lethality due to disruption of axial patterning with missing mesoderm and primitive streak formation (Augustin et al., 2013; Fu et al., 2009).

Embryonic stem cells (ESCs) are widely used to study early differentiation processes (Posfai et al., 2014). They also hold promise for therapeutic approaches in the field of regenerative medicine (Dressel, 2011; Dressel et al., 2008; Song et al., 2015; Tang and Drukker, 2011). Yet, immune rejection resulting from mismatch histocompatibility is a potential limitation of stem cell-based therapies, restricting the rate of successful transplantation (Zhao et al., 2011; Jin et al., 2015). Moreover,

* Corresponding author at: University of Applied Sciences, Faculty of Biotechnology and Bioinformatics, Am Hofgarten 10, Freising 85354, Germany.
E-mail addresses: i.augustin@dkfz.de, iris.augustin@hswt.de (I. Augustin).

http://dx.doi.org/10.1016/j.scr.2016.10.010

ESC transplantation may hold the risk of teratoma formation because undifferentiated ESCs give rise to teratomas, which resemble benign tumors that consist of tissues derived from the three embryonic germ layers (Przyborski, 2005; Lee et al., 2013). Accordingly, teratoma formation assays need to be performed to confirm ESC pluripotency in a complex *in vivo* environment. Teratoma assays are also pursued as a model to investigate the crosstalk between ESCs and stromal cells (Przyborski, 2005; Dressel, 2011). We previously generated Evi-overexpressing mouse ESCs (Evi-GOF) *via* knockin into the ROSA26 locus to study Wnt secretion in ESCs (Augustin et al., 2012). Evi-GOF ESCs showed enhanced Wnt activity, which had no effect on ESC pluripotency and viability. Teratoma experiments with Evi-GOF ESCs confirmed pluripotency characterized by meso-, *endo*- and ectodermal lineage differentiation although Evi-GOF ESCs revealed a preference for cardiomyocyte differentiation. Based on these findings, the present study was aimed at investigating Evi during teratoma formation in order to clarify the role of Wnt secretion in teratoma–stroma interactions in a definite genetic setting.

2. Results

2.1. Evi overexpression leads to larger teratomas in syngeneic mice and promotes cardiogenic differentiation

ESCs express a repertoire of Wnt ligands, which activate canonical and non-canonical Wnt signaling cascades. As a cargo-receptor, Evi acts as a gatekeeper to release or block Wnt secretion. Increased levels of the cargo-receptor have been detected in different tumor entities (Augustin et al., 2012; Voloshanenko et al., 2013; Lu et al., 2015). Accordingly, Evi overexpression (Evi-GOF) leads to a global increase of secreted Wnt proteins and represent a model of enhanced Wnt signaling. Evi-GOF ESCs ectopically express Evi-YFP, which is localized to the secretory pathway (Fig. 1A). FACS-based analysis of ESCs confirmed the surface expression of Evi-YFP, indicating proper cellular trafficking of Evi-YFP (Fig. 1B). Western blots of ESC supernatants showed increased Wnt5a/5b secretion of Evi-GOF ESCs, which was abolished in the presence of LGK947 (Fig. 1C). Previous results showed an increased Wnt-reporter activity of Evi-GOF ESCs (Augustin et al., 2012). Accordingly, LRP6, the co-receptor of Frizzled, revealed higher phosphorylation in Evi-GOF ESCs compared to control cells, which was prevented after LGK947 treatment (Fig. 1D). Likewise, expression of the Wnt target gene *Axin2* was increased (Fig. 1E).

Wnt signaling has been shown to support ESC maintenance. Therefore, we investigated the expression of the pluripotency markers *Oct4*, *Nanog*, *Sox2*, *Rex1* as well as Epi-stem cell marker *Claudin1* and early differentiation markers *CD133* and *Fgf5* (Fig. 1F, G). Enhanced Wnt secretion resulted in no significant changes in their gene expression. Similarly, protein expression of Nanog, SSEA1 and Oct4 was unchanged based on FACS analysis indicating no major alterations in the pluripotency network of Evi-GOF ESCs. Moreover, enhanced Wnt secretion had no effect on the viability and growth of cultured Evi-GOF ESCs (Fig. 1H). Similar growth curves were observed in the presence of low serum concentrations (5%) or in the absence of LIF (data not shown).

Subcutaneous injection of Evi GOF and control ESCs in syngenic recipients (129P2/OlaHsd) were performed to generate teratomas and analyze the differentiation potential if ESC *in vivo*. Monitoring of tumor growth over time revealed larger tumors in Evi GOF ESCs (Fig. 2A). Evi-YFP expression was detected in Evi-GOF teratoma sections (Fig. 2B). Labeled cells showed prominent perinuclear and surface staining and were clearly distinguishable from unlabeled host-derived stromal cells (Fig. 2B). Histological analysis of teratomas was performed to assess the differentiation potential of the injected ESCs. H&E stained sections showed characteristic structure of endo-, meso- and ectodermal differentiation (Fig. 2C). Proliferation of tumor cells was not altered as evidenced by EdU-incorporation experiments (Fig. 2D). Active caspase-3 labeling showed reduced apoptosis rate in Evi-GOF teratomas. However, it was not significant. (Fig. 2E).

In order to understand the differences between *in vitro* and *in vivo* growth, we performed expression profiling of teratomas from Evi-GOF and control ESCs. RNA from teratomas was isolated and analyzed by array-based expression profiles to study cellular and molecular mechanisms underlying Evi-GOF teratoma development. A set of 18 genes was significantly upregulated and 123 genes were downregulated in Evi-GOF teratomas (absolute value of $\log_2$ fold change >1; adj. p-value < 0.05) (Fig. 3A). Tissue-related expression analysis of the upregulated genes based on TiGER profiles (http://bioinfo.wilmer.jhu.edu/tiger/) showed that 61% of the genes had a muscle and heart association, whereas 39% of the genes were ubiquitously expressed or had other tissue preferences, supporting the concept that Evi-GOF ESCs reinforced mesodermal differentiation to result in enhanced muscle development (Fig. 3B). Similar results were reported after Wnt1 overexpression (Weisel et al., 2010) or sustained treatment of ESCs with Wnt3a or GSK-inhibitor (Bakre et al., 2007). The list of upregulated genes related to muscle and heart development is summarized in Fig. 3C.

2.2. Reduced expression of immune-modulatory genes in Evi-overexpressing teratomas

Among the downregulated genes, the highest enrichment was observed in genes categorized as immunity and defense (43% of the downregulated genes) as well as signal transduction (30% of the downregulated genes) (Fig. 3D). Similarly, genes involved in T- and B-cell-mediated immunity, as well as innate immunity were differentially expressed suggesting an altered immune response (Fig. 3D). Among others, the genes coding for three CD3 chains (*CD3γ*, *CD3δ*, *CD3ε*) – part of the TCR-CD3 complex – were downregulated about 3-fold (Fig. 3E). The *CD79b* antigen, part of the B lymphocyte antigen receptor, was also downregulated (Fig. 2E). Next, we studied if surface markers involved in T cell activation and survival were differentially expressed in Evi-GOF and control teratomas. The B7 family members CD80 (B7–1) and CD86 (B7–2) work in tandem to activate T cells *via* binding to CD28 co-receptor. Following activation, the inhibitory receptor CTLA-4 is induced in T cells, which compete with CD28 for CD80 and CD86 ligands and provided an inhibitory signal to stop T cell activation. In contrast to *CD86*, *CD80* expression was reduced in Evi-GOF teratomas suggesting an imbalance in T cell activation in Evi-GOF tumors compared to controls (Fig. 3F). However, *CTLA-4*, *PD-L1* and *MHC* class *II* and *I* markers were not significantly changed, suggesting that no major differences regarding tumor recognition by the immune system were apparent (Fig. 3F). Imunohistochemical analysis against MHC class II revealed heterogeneous but similar staining pattern (Fig. 3G). This result might be due to the fact, that embryonic stem cells are non-cancer cells but develop benign teratomas composed of cells resembling normal derivatives and therefore, other than tumor cells, do not use mechanisms to become less immunogenic. Further detailed quantitative analysis on marker gene expression would be necessary to confirm this conclusion.

2.3. Evi overexpression affects teratoma-immune-cell crosstalk

Expression studies showed that Evi-overexpressing ESCs favored a cardiomyocyte gene expression profile, and that immune regulatory genes were downregulated. Enhanced muscle differentiation might be associated with an altered immune response indicating that the cardiomyocyte lineage itself and not the Wnt overexpressing teratoma cells in general is linked to reduced immune cell crosstalk. Therefore, we compared the expression of the cardiomyocyte marker *troponin C type 1* (*Tnnc1*) and the skeletal muscle marker *myosin heavy chain 8* (*Myh8*) as a surrogate marker of cardiomyocyte differentiation, with the expression pattern of the immune cell markers *CD3* (T cells) and *CD19* (B cells). The correlation (R^2) between *Myh8* and *Tnnc1* with *CD3* or

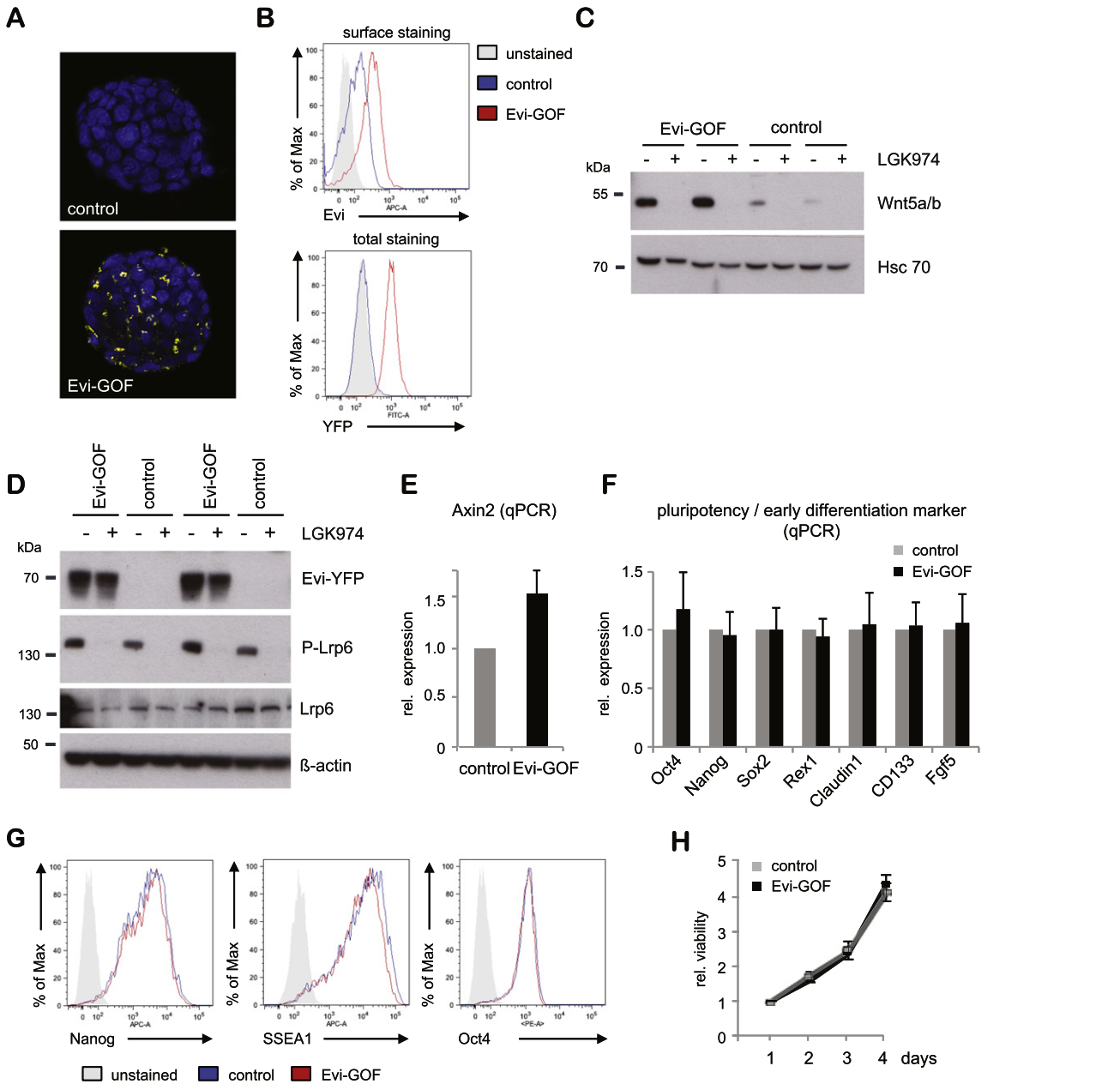

Fig. 1. Evi-GOF ESCs have enhanced Wnt signaling activity with unaltered cell viability. (A) Evi-GOF and control ESC colony. Evi-YFP expression was localized to the secretory pathway and the plasma membrane. DAPI stained the nucleus. (B) FACS analysis of unpermeabilized and permeabelized ESCs with an antibody against Evi or GFP confirmed Evi-YFP expression on the cell surface. (C) Western blot of control and Evi-GOF ESC culture supernatants generated in the presents or absence of LGK974 were incubated with antibodies against Wnt5a/b and Hsc70 for loading control (D) Western blot of control and Evi-GOF ESC lysates incubated with antibodies against YFP, phospho-LRP6 and LRP6 dependent on LGK974 treatment. β-actin was used as a loading control. (E, F) RT-PCR analysis of control and Evi-GOF ESCs for indicated genes 48 h after seeding. (G) FACS analysis of Evi-GOF and control cells with indicated antibodies. Grey area represents unstained cells. (H) Relative viability of Evi-GOF and control cells over time. ESCs were depleted of MEFs and incubated in the presence of LIF-containing medium. Data represent mean ± SD of 3 independent experiments. Similar results were obtained with an independent ESC line.

CD19 was not significant indicating that the expression of immune system markers was not affected by altered teratoma differentiation in the Evi-GOF tumors (Fig. S1A).

As shown above, Evi-GOF teratoma were larger than control tumors (Fig. 2B). We therefore analyzed whether the infiltration of immune cells in general was dependent on teratoma size. FACS-based analysis of control teratoma tissue was performed after 27 days of growth. We analyzed the percentage of $CD45^+$ and $CD3^+$ populations from total teratoma cells harvested from tumors of various sizes ranging from 0.4 mg to 0.9 mg (Fig. S1B) and found no significant correlation between the number of $CD45^+$ and $CD3^+$ cells and tumor weight.

Given that Evi-GOF teratomas showed predominately down-regulation of genes, which were functionally related to immunity and defense, we hypothesized that Evi expression may affect immune cell infiltration. Therefore, we FACS-profiled the leukocytes that had infiltrated the teratomas. We found that the number of $CD45^+$ cells was 2-fold higher in the control teratomas compared to Evi-GOF teratomas (Fig. 4A). The data indicates that constitutive overexpression of Evi in ESCs suppressed teratoma immune cell infiltration.

To further investigate the frequency of leukocyte subpopulations in Evi-GOF and control teratomas, we performed FACS profiling distinguishing the infiltrated cell numbers of lymphocytes and myeloid populations. $CD45^+$ subpopulation analysis revealed about 50% reduction in $CD3^+$ T cells as well as $CD19^+$ B cells, whereas $F4/80^+$, $Gr1^-$ macrophages, $Gr1^+$, $CD11b^+$ granulocytes and $CD49b^+$, $CD3^-$ NK cells were not significantly altered (Fig. 4A). The ratio of T- to B cells

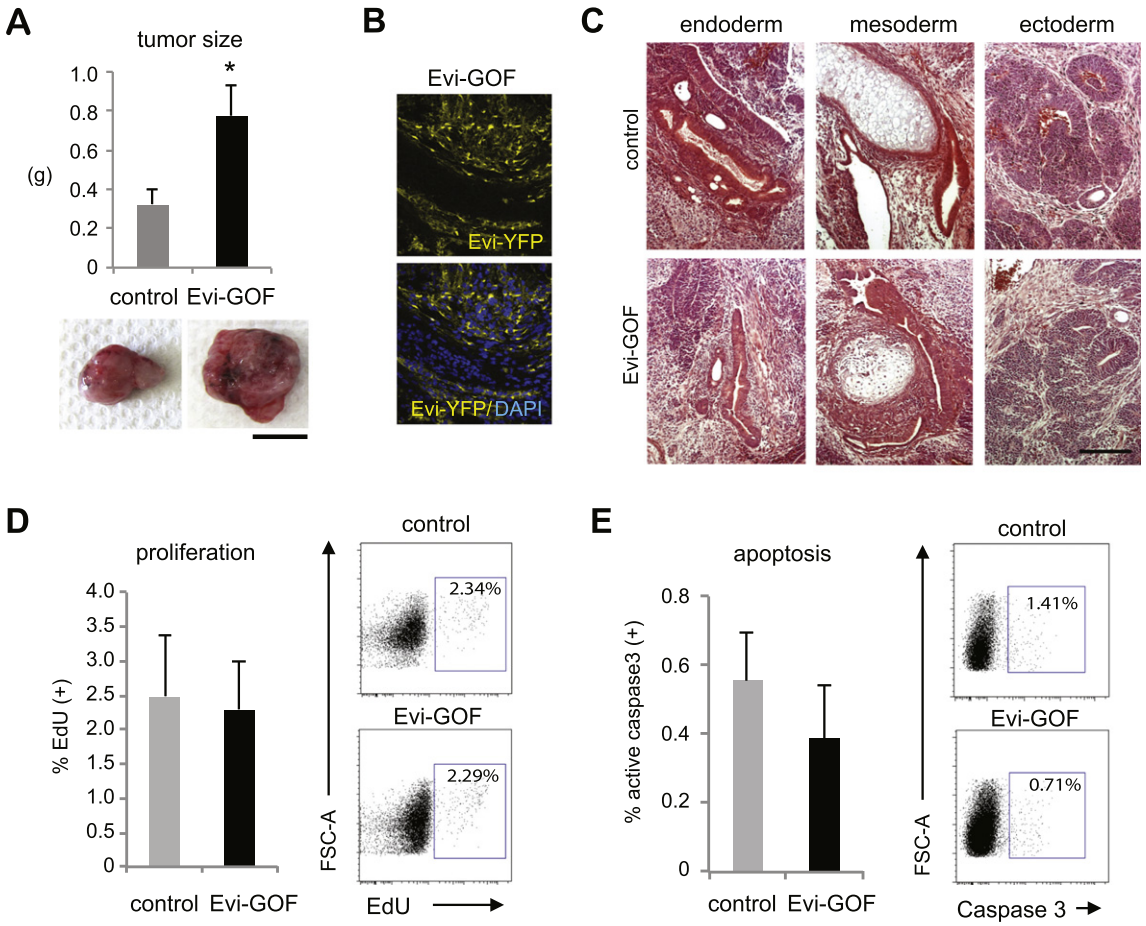

Fig. 2. Teratomas from Evi-overexpression and control ESC. (A) Tumor size after 27 days of teratoma growth in 129P2/OlaHsd mice (control $n = 14$, Evi-GOF $n = 10$) Data represents SEM of 2 independent experiments (upper panel). Representative pictures of Evi-GOF and control teratomas (scale bar 1 cm) (lower panel). (B) Representative section of Evi-GOF teratomas stained with an anti-GFP antibody. (C) Teratoma sections from Evi-GOF and control tumors stained with H&E (scale bar 100 μm). (E) Analysis of EdU-labeled cells of control and Evi-GOF tumors. (D) Analysis of active caspase3(+) cells in Evi-GOF and control teratomas. Data represent mean ± SD of 3 independent experiments, 2 independent clones per genotype were tested. $^{\star}p < 0.05$.

in Evi-GOF tumors was unaltered compared to control tumors (data not shown), indicating that both T-and B cells were affected. Immunohistochemical analysis of $CD3^+$ cells confirmed the reduced T-cell recruitment in Evi-GOF teratomas (Fig. S2A).

If the tumor-promoting role of Wnt secretion relied on reduced lymphocyte infiltration, persistance and/or impaired T cell activation, the growth advantage of Evi-GOF teratomas grown in immune-compromised Nod/SCID mice, which are deficient in mature T and B cells, should be lost. Indeed, in Nod/SCID mice, tumor sizes (and lymphoid immune infiltration) of Evi-GOF- and control tumors were comparable, supporting the hypothesis that exacerbated Wnt secretion impaired the antitumor immune surveillance of the adaptive immune system (Fig. 4B, C), rather than conferring an intrinsic growth advantage. Subsequent analysis of $CD4^+$ and $CD8^+$ T cell subsets revealed similar distribution in Evi-GOF and control tumors (Fig. 4D). The $CD4^+/CD8a^+$ ratio was also indistinguishable in both teratoma types (Fig. S2B). Further analysis of T cells regarding $CD4^+$ effector memory (T_{EM}: $CD44^{hi}$, $CD62L^-$), central memory (T_{CM}: $CD44^{hi}$, $CD62L^+$), and naïve (T_N: $CD44^-$, $CD62L^+$) subpopulations showed no changes in Evi-GOF teratomas compared to controls (Fig. 4E). The profiling of $CD8^+$ cells revealed no significant alterations in T_{EM} and T_{CM} subpopulations whereas the fraction of naïve cells in Evi-GOF teratomas was about 50% reduced (Fig. 4F). Similarly, the activated T cell populations expressing $CD69^+$ were not altered in Evi-GOF teratomas (Fig. S2C). The ability of $CD4^+$ T cells to exert effector functions depends on their differentiation. Wnt/β-catenin signaling regulates lineage fate decisions in both the thymus and in peripheral lymphoid tissue and it enhances the survival of regulatory T (Treg) cells (Ding et al., 2008) (Yu et al., 2010) (Notani et al., 2010). Interestingly, the fraction of $CD4^+$, $CD25^+$, $FoxP3^+$ regulatory T cells was significantly increased in Evi-GOF teratomas (Fig. 4G). Similarly, the frequency of IL17-producing $CD4^+$Th17 cells was elevated in Evi-GOF teratomas supporting the idea that Wnt signaling enhanced Th17 differentiation (Fig. 4H) (Ma et al., 2011; Dai et al., 2016; Muranski et al., 2011). Next, we asked for extracellular factors responsible for Th17 differentiation. Stimulating naïve T cells with TGF-β and IL6 is sufficient to induce IL17 producing cells (Ma et al., 2011). Q-PCR analysis of IL6 expression in Evi-GOF and control tumors revealed almost 2-fold upregulation of IL6 in Evi-GOF teratomas suggesting that IL6-Stat3 signaling cascade is more pronounced in Evi-GOF teratomas and might contribute to enhanced Th17 differentiation.

In order to investigate the correlation of Evi expression and leucocyte markers in tumor patient biopsies we performed expression analysis of cancer profiles. Using the R2 - Genomics Analysis and Visualization Platform we analyzed the co-expression of *Evi* and leucocyte markers (*CD45*, *CD3ε*, *CD3δ*, *CD4*, *CD8a*, *F4/80*, *CD19*) in colon cancer patient cohorts (Tumor Colon Sieber 315 Mas5.0-u133p2, Fig. S3A). Our analysis revealed that tumor samples with high *Evi* expression showed low expression of leukocyte markers indicating that Wnt signaling interferes with the tumor-immune crosstalk in mouse and human tumor tissues. Similar results were obtained with a second colon cancer database

A

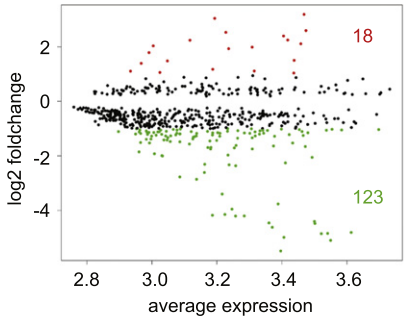

B

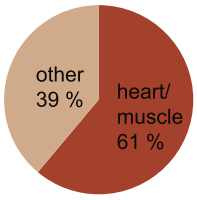

C

upregulated/muscle-related genes

Symbol	log2FC	adj. p-value
Myh8	3.24	0.018
Csrp3	2.62	0.026
Tnnc1	2.60	0.047
Sln	2.40	0.021
Actn2	2.28	0.037
Des	2.11	0.029
Ankrd2	1.79	0.048
Cox6a2	1.50	0.033
Ankrd1	1.48	0.046
Myoz2	1.39	0.046
Nkx2.1	1.06	0.035

D

Panther analysis of downregulated genes

Term	% genes	p-value
Immunity and defence	43.30	3.0 E-21
T-cell mediated immunity	16.49	2.4 E-13
Natural kill cell mediated immunity	6.19	2.0 E-05
Complement-mediated immunity	5.15	1.2 E-04
Receptor protein tyrosine kinase signaling pathway	6.19	3.3 E-03
Macrophage-mediated immunity	5.15	4.6 E-03
B-cell- and antibody-mediated immunity	7.22	7.3 E-03
Signal transduction	29.90	2.1 E-02

E

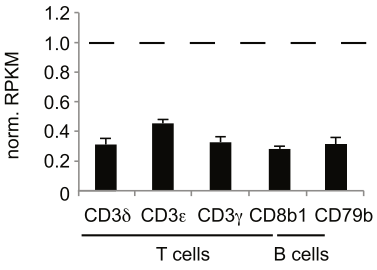

F

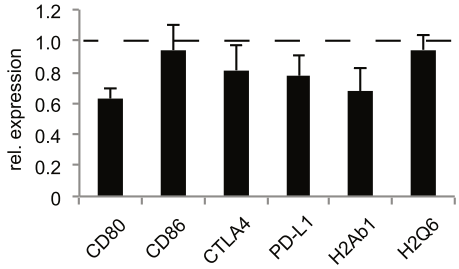

G

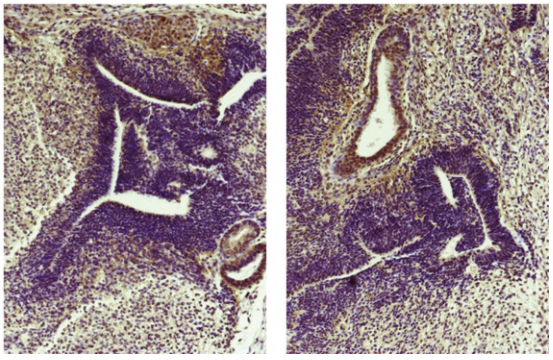

Fig. 3. Expression profiling of Evi-GOF teratomas. (A) Scatter plot showing differentially regulated genes identified by Array-Express profiling of teratoma RNA obtained from 5 tumors per genotype. Genes with $\log_2$ fold changes >1, adjusted *p*-values <0.05 are labeled in color. (B) Overview of TiGER analysis of upregulated genes in Evi-GOF tumors. (C) List of upregulated genes in Evi-GOF teratomas related to muscle differentitaion. (D) Panther analysis of downregulated genes was performed to identify changes in signaling pathways. (E) Expression profiling of downregulated genes obtained by Array-Express analysis ($n = 5$). Values are normalized to control teratomas. (F) qPCR analysis of indicated genes normalized to control tumors (control $n = 25$; Evi-GOF $n = 27$). Data represents mean ± SEM of 7 experiments. (G) Teratoma section stained with an antibody against MHC II.

(Tumor Colon EXPO 355 Mas5.0-u133p2) and ovarian, pancreatic and breast cancer studies (data not shown) suggesting a comprehensive role of Wnt secretion in cancer immune regulation.

The present study was based on a novel mouse teratoma model. Accordingly, we analyzed *Evi* expression in a human Korkola Seminoma tumor data set, which includes different germ cell tumor classes (embryonal carcinoma, mixed germ cell tumor, seminoma, teratoma, yolk sack tumor; TCGA, Oncomine) (Fig. S3B). *Evi* was upregulated in teratomas (fold change 3.579, *p-value* 3.55E-8) suggesting that teratomas reflect another tumor entity with high Wnt importance. Further studies are necessary to decipher a potential role of Evi in human teratoma immune cell recruitment.

3. Discussion

ESCs have the potential to differentiate in all types of cells. *In vivo* application of undifferentiated ESCs leads to teratoma formation (Dressel et al., 2008; Song et al., 2015). A recent screening study identified an involvement of Wnt signaling in the transition from benign to malignant teratocarcinoma growth (Liu et al., 2012). Moreover, upregulated Evi expression was found in human teratomas supporting the hypothesis that Evi may contribute to germ cell tumor progression. The Evi-transgenic ESC line reported in this study provides a novel research tool to study teratoma formation. Evi-GOF teratomas showed enhanced tumor growth demonstrating a tumor-promoting role of Evi in ESCs.

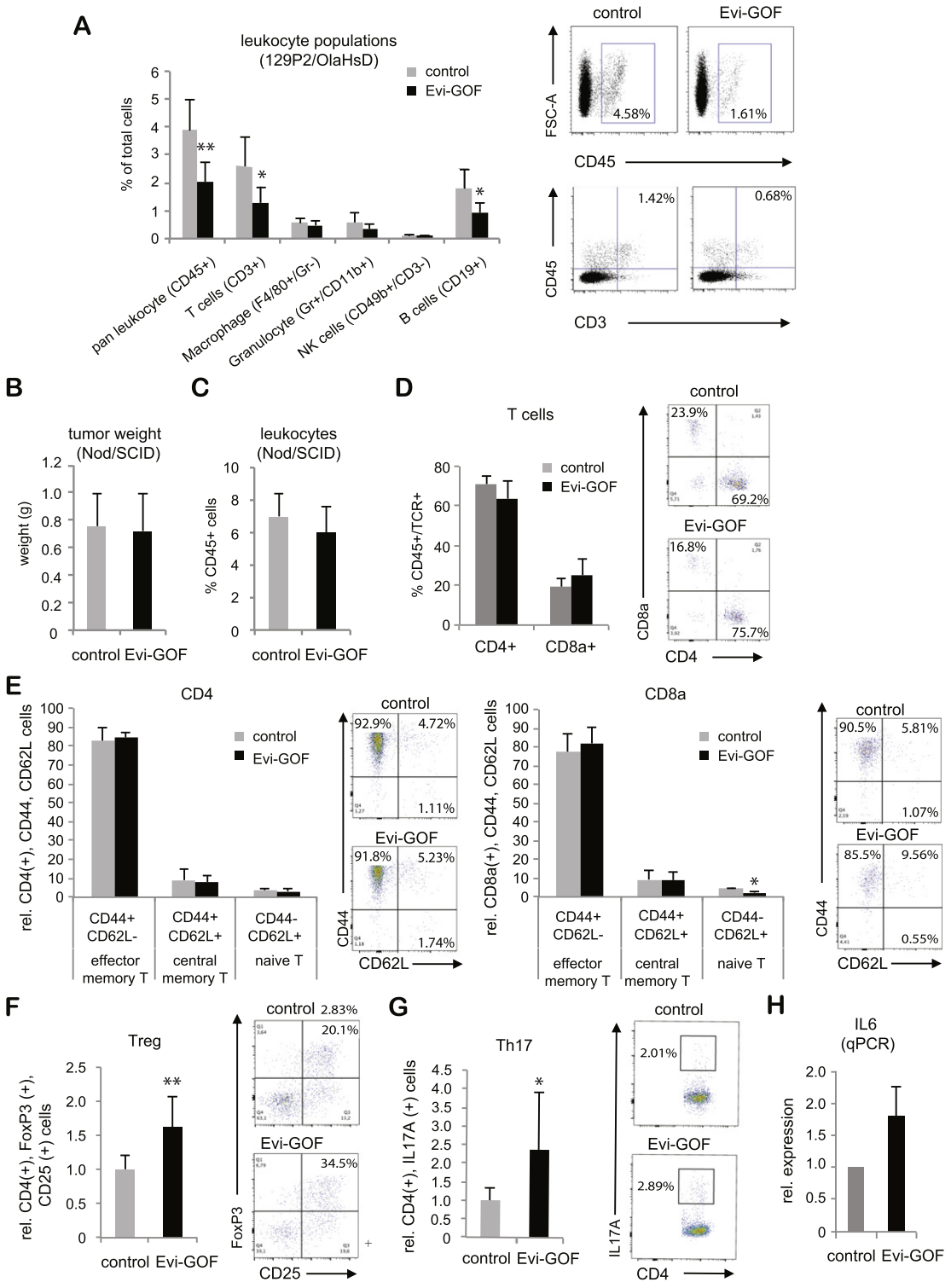

Fig. 4. Evi-GOF teratomas recruit fewer T and B cells. (A) FACS-based analysis of dissociated teratomas of Evi-GOF and control ESCs injected in 129P2/OlaHsd mice after 27 days of transplantation. Cells were gated according to the indicated markers. (control, $n = 7$; Evi-GOF, $n = 9$). (B) Teratoma weight of Evi-GOF and control ESCs injected in Nod/SCID mice (harvest after 27 days) ($n = 15$). (C) FACS-based analysis of $CD45^+$ cells in Evi-GOF and control tumors injected in Nod/SCID mice after 27 days of transplantation. ($n = 15$). (D) FACS-based analysis of $CD4^+$ and $CD8^+$ leukocytes of Evi-GOF and control tumors (control, $n = 7$; Evi-GOF, $n = 6$). (E) FACS-based analysis of $CD4^+$ or $CD8^+$ populations against CD44 and CD26L expression (control, $n = 24$; Evi-GOF, $n = 25$). (F) FACS-based analysis of $CD4^+$ cells against CD25 and FoxP3 (control, $n = 21$; Evi-GOF, $n = 17$). (G) FACS-based analysis of $CD4^+$ cells against IL17 (control, $n = 11$; Evi-GOF, $n = 13$). (H) qPCR analysis of indicated genes normalized to control tumors (control $n = 17$; Evi-GOF $n = 22$). Representative FACS plots were shown on the right. Data represents representative analysis (A, C) and mean ± SD of 2–4 experiments (D–G).

Correspondingly, previous experiments in glioblastoma and colorectal tumor cells had shown that loss of Evi resulted in inhibition of tumor growth after xenotransplantation (Augustin et al., 2012; Voloshanenko et al., 2013).

The host immune response has been identified as a critical regulator of tumor development and progression (Dunn et al., 2004; Fridman et al., 2013; Hadrup et al., 2013). Several types of immune cells participate in immunosurveillance by direct killing or production of cytokines. Our

expression profiling experiments revealed that the majority of genes related to immunity and defense were significantly downregulated in Evi-GOF teratomas. Accordingly, less $CD45^+$ leukocytes had infiltrated Evi-GOF teratomas. Most notably, we observed a 50% reduction of $CD3^+$ T cells in Evi-GOF teratomas. Low densities of both $CD8^+$ cytotoxic T cells and $CD45RO^+$ memory T cells are associated with poor clinical outcome (Fridman et al., 2013; Becht et al., 2014; Hadrup et al., 2013). The results of our teratoma experiments support a model whereby high Wnt activity facilitated the escape from the anti-tumor immune control by T cell exclusion. Recent results on Wnt/β-catenin signaling in melanoma have revealed a correlation of canonical Wnt signaling with lack of T-cell infiltration in mouse models as well as in human patient biopsies suggesting a similar role of Wnt signaling in different types of tumors (Spranger et al., 2015). Our analysis revealed no overt changes in T cell activation or effector differentiation, indicating that excessive Wnt signaling impairs T cell recruitment and/or tumor infiltration, rather than intratumoral T cell activation. Alternatively, the moderate Evi overexpression in ESCs *via* the Rosa26 promoter was insufficient to challenge the balance of these T cell subsets. Regardless of the exact mechanism, elevated Wnt levels promote increased tumor growth and this effect is mediated through attenuated immune surveillance. The role of Wnt signaling in mature T cell differentiation is still controversially discussed. Recent publications using pharmacological or genetic approaches support a role for β-catenin as well as the β-catenin downstream transcription factor TCF-1 (transcription factor 7) in memory T cell development (Gattinoni et al., 2009; Zhao et al., 2010). Whereas other reports showed that expression of stabilized or deleted β-catenin was dispensable in functional memory T cell differentiation (Prlic and Bevan, 2011; Driessens et al., 2010). It is of note that TCF-1 can be activated independently of β-catenin cooperation and therefore does not reflect in all cases exclusive Wnt response (Grumolato et al., 2013; Sprowl and Waterman, 2013). Similarly, studies addressing Wnt/β-catenin signaling in Treg and Th17 function showed on the one hand that stable β-catenin expression in Tregs supports Treg survival and immune response (Ding et al., 2008), whereas TCF-1 deficient mutants revealed stronger suppressive ability of (van Loosdregt et al., 2013). Our teratoma analysis showed an increase in $CD4^+CD25^+FoxP3^+$ Tregs population in Evi-GOF tumors indicating that enhanced Wnt secretion supports Treg availability. Further experimental analyses will be necessary to clarify whether this phenotype correlates with β-catenin or β-catenin-independent Wnt signaling in T cell populations. Tregs suppress inflammatory mechanisms and thereby attenuate inflammation-associated tumor progression. Otherwise regulatory T cells also inhibit anti-tumor T cell responses, thereby supporting cancer escape from immune surveillance. These different functions are probably driven by different Treg subsets, which might depend on the cancer type and mutation status. (Blatner et al., 2012; Keerthivasan et al., 2014). Recent reports showed that active Wnt/β-catenin signaling in Tregs correlates with promotion of colon cancer (Keerthivasan et al., 2014). Further studies are necessary to address this issue in other Wnt-related cancer settings. Moreover, several reports exist, which delineate a role of Wnt signaling in Th17 differentiation during T cell development and mature T cell differentiation (Ma et al., 2011; Dai et al., 2016; Muranski et al., 2011). Our results showed an increase in IL17 producing $CD4^+$ T cells in Evi-GOF teratomas indicating that enhanced Wnt secretion is involved in elevated Th17 response. The supportive or inhibitory role of Th17 in malignancy is still a matter of debate suggesting that Th17 cells play a dynamic role in cancer immunity depending on the type of inflammatory response and cancer (Martin et al. 2012; Wang et al., 2009; Iida et al., 2011). Recent reports showed that constitutive activation of β-catenin promotes chromatin accessibility and target gene expression for Th17 commitment, which sustained pathogenic inflammation and predispose to cancer (Keerthivasan et al., 2014). Our phenotypical analyses tend towards the same direction. Nevertheless additional studies are necessary to enroll a more detailed leukocyte population analysis including expression pattern of target genes and cytokines as well as Wnt signal activity.

Previous studies have focused on the analysis of tumor infiltrating T cells. In turn, much less is known about the role of B cells in modulating the immune response to solid tumors (Nelson et al., 2010). It has been shown for melanoma and several other types of tumors that B cell density correlates with T cell density indicating that B cells support the antitumor immune response (Zirakzadeh et al., 2013). Accordingly, our study also revealed a concomitant reduction of tumor-infiltrating T and B cells.

In conclusion, the identification of Wnt secretion as a regulator of teratoma growth and immune cell infiltration may have profound impact for the molecular understanding of tumor - immune cell crosstalk with possible translational relevance. Future work will have to unravel the underlying signaling mechanisms regulating the escape from the anti-tumor immune response in order to contribute to the further advancement of cancer immunotherapies.

4. Material and methods

4.1. Cell culture, cell lines, constructs, generation of stable ESC

Evi-GOF ESCs were generated and maintained as previously described (Augustin et al., 2012) (genetic background: 129P2/OlaHsd). 6 independent lines were generated. At least two lines per genotype were investigated to exclude clone-specific artifacts. Briefly, ESCs were cultured on mitomycin C inactivated feeder cells (MEFs) in LIF supplemented ESC medium (DMEM high glucose (Gibco) supplemented with 15% FCS (PAN Biotech), 1% Penicillin / Streptomycin (Invitrogen), 2 mM Glutamine (Invitrogen), 100 μM β-mercaptoethanol (Sigma), 1 mM MEM-sodium pyruvate (Invitrogen), 1% non-essential amino acids (Invitrogen), and 1000 U/ml Leukemia Inhibitory factor (LIF, Millipore)) (Lin and Talbot, 2011). ESCs were passaged on gelatine-coated plates to deplete MEFs and used for experiments after 3–5 passages on gelatine-coated plates. ESCs were cultured at 37 °C, 5% CO_2 and passaged 1:3 every 2–3 days.

4.2. Cell viability

To assess cell viability, 1000 cells were plated in 10 replicates on gelatine-coated 384-well plates in LIF containing medium and viability was measured at indicated time points using CellTiter-Glo (Promega) according to the manufacturer's protocol.

4.3. Animal experiments

Viable ESCs (3×10^6 cells in 100 μl PBS) were injected into the dorsal flank of 129P2/OlaHsd or Nod/SCID mice (age of 6–10 weeks). Teratomas were isolated 27 days after transplantation. For *in vivo* analysis, mice were injected i.p. with EdU (20 μg/g mouse) 2 h before sacrifice. Animal welfare and experimental procedures were performed in accordance to German animal protection law and were approved by the Regierungspräsidium Karlsruhe, Germany (AZ 35–9185.81/230/11).

4.4. Immunohistochemistry

Following deparaffination, antigen retrieval was performed by heating sections at 98 °C for 10 min in 10 mM citrate buffer (pH 6.0). To block endogenous peroxidase, sections were treated with 3% H_2O_2 for 20 min. After blocking with avidin/biotin blocking (Dako) solution at room temperature for 1 h. Sections were incubated with CD3 primary antibodies in blocking solution overnight at 4 °C. Following washings with PBS, the slides were incubated with HRP-labeled secondary antibody for 3 h at room temperature. Incubation with Avidin/Biotin complex (Dako) was done for 30 min at room temperature, followed by incubation with diaminobenzidine substrate until brown color appeared. Counterstaining was performed with hematoxylin. Sections

were mounted in Histofluid (Engelbrecht), and photographed using a Zeiss Axioskop 40 microscope.

4.5. FACS analysis

Teratomas were mechanically minced into small pieces using scalpels, followed by a digestion step for 2 h at 37 °C in collagenase D at concentration of 2 mg/ml in RPMI medium supplemented by 10% FCS, Penicillin/Streptomycin (Invitrogen) and 2 mM Glutamine (Invitrogen). Gentle pipetting was performed during digestion. Cell suspensions were filtered through a 70 μm nylon filter mesh (BD), washed in PBS once, counted and processed for antibody staining and FACS analysis. For IL17 staining cells were stimulated with cell stimulation cocktail plus transport inhibitors (ebioscience) for 4 h at 37 °C. FoxP3 stainings were performed according to FoxP3/Transcription Staining Buffer Set (ebioscience). Single cell suspensions from teratomas or cultured cells were stained with antibodies diluted in PBS containing 5% FCS for 45 min at 4 °C. For intracellular labeling, cells were permeabilized either with 0.2% Triton X100/PBS for 5 min before incubation with conjugated primary antibodies or according to FoxP3/Transcription Staining Buffer Set. Secondary antibody staining was performed for non-fluorescent conjugated primary antibody. After staining, cells were fixed with 2% PFA for 10 min, washed and subsequently processed for FACS analysis. Proliferation and apoptosis assays were performed using EdU-Click iT reagent (Invitrogen) and PE Active Caspase-3 Apoptosis Kit (BD pharmingen), according to the manufacturer's instruction. Fluorescence data were obtained with a FACS LSRII (BD) with FACS Diva software. Data were subsequently analyzed using Flow Jo 10.1 software. Antibodies are listed in Table S1, 2.

4.6. Western blot analysis

Cell pellets were lysed in urea buffer containing 8 M urea in PBS. Lysates were incubated on ice for 30 min and centrifuged at 3000 g for 15 min at 4 °C. Supernatants were collected and protein concentrations were determined by BCA (Perbio, Thermo Scientific) according to the manufacturer's instructions. Proteins (15 μg) were supplemented with 5× Laemmli buffer and heated for 10 min at 80 °C. Cell lysates were separated on 4–12% NuPage gradient gels Bis-Tris (Life Technologies) and transferred to PVDF membranes (Millipore, Merck Biosciences). In order to enrich Wnt proteins in cell culture supernatants medium was centrifuged at 15,000 g for 10 min to get rid of debris. Triton X100 (1% final) was added to the medium followed by addition of 50 μl blue sepharose beads (GE Healthcare) per 10 ml medium. Mix was incubated overnight at 4 °C. After washing the beads three times (150 mm KCL, 50 mM Tris-Cl, 1% Triton X100) the beads were resuspended in 2× Laemmli buffer and heated for 5 min at 96 °C. Supernatants were loaded on 4–12% NuPage gradient gels Bis-Tris (Life Technologies) and transferred to PVDF membranes (Millipore, Merck Biosciences). Membranes were blocked in 5% non-fat dry milk/PBS incubated overnight at 4 °C with primary antibodies. Blots were then incubated with corresponding HRP–conjugated secondary antibodies (Sigma-Aldrich). Antibodies are listed in Table S1, 2.

4.7. RNA, RT-PCR and expression profiling

Total RNA was extracted from ESCs and teratomas using RNAeasy extraction kit (Qiagen) according to the manufacturer's instructions. Reverse transcription and quantitative PCR was performed with 25 ng cDNA and LightCycler 480 Probes Master as described (Roche) (Primers were listed in Table S2). Relative mRNA expression was calculated as a fold change *versus* control. Teratomas were harvested 27 days after ESC injection and pulverized thoroughly in a mortar cooled with liquid nitrogen for further extraction of RNA.

Total RNA was isolated from each of the 10 teratoma samples using RNAeasy Kit (Qiagen) and labeled cRNA were prepared according to Illumina TotalPrep-RNA amplification protocol (P/N IL1791M, Life Technologies). 1.5 μg cRNA were hybridized for 17 h at 58 °C on Illumina BeadChip Sentrix array (mouse WG-6 v2.0) according to Standard Illumina Hybridization protocol (#11322355). Gene expression microarrays were scanned using the Illumina iScan-Scanner according to Standard Illumina Scanning protocol, using BeadStudio software (v3.2). The limma package (v3.2.1), part of the Bioconductor/R package, was employed to test for differential expression (Wettenhall and Smyth, 2004). This test assumes a linear model for gene expression levels. The differential expression test between Evi-GOF and control teratoma samples is based on the null hypothesis that the expression values of a gene in the samples come from the same distribution and results in *p*-values for each gene. A simple design matrix was created to fit a linear model to each gene expression value. An empirical Bayes method was used to moderate standard errors and estimate log fold change from the data, and a moderated t-statistic was used to assess differential expression. Genes which had an adjusted (Benjamini–Hochberg} p-value < 0.05 and absolute value of $\log_2$ fold change greater than 1 were regarded as differentially expressed, and used for further PANTHER (Mi et al., 2005) (http://www.pantherdb.org/) and TiGER (Liu et al., 2008) (http://bioinfo.wilmer.jhu.edu/tiger/) analysis. Analysis of the correlation of *Evi* and leukocyte markers was performed with R2: Genomics Analysis and Visualization Platform. http://hgserver1.amc.nl/cgi-bin/r2/main.cgi?&species=hs. *Evi* expression in germ cell tumors was analyzed in Oncomine, www.oncomine.com.

4.8. Statistical analysis

Unless otherwise indicated, data are expressed as mean ± SD. Statistical significance was calculated by a two-tailed Student's *t*-test with unequal variance. A p-value of <0.05 was considered statistically significant and marked in comparisons by asterisks. One asterisks represent p-values of <0.05. Two asterisks mark p-values of <0.01.

4.9. Accession numbers

Expression profiling data is submitted to ArrayExpress E-MTAB-3995.

Authorship contribution

I.A. and M.B. designed the study. I.A., D.D. J.H. performed research, analyzed and interpreted data. E.R. performed analysis on expression profiles. F. B. supported experimental design and discussion. I.A. and M.B. wrote the manuscript.

Acknowledgements

We gratefully acknowledge support by the DKFZ FACS core facility, the Genomic and Proteomics Core Facility for expression analysis, the animal department and transgenic unit for animal support. We thank G. Vollert for technical support, H. G. Augustin and the members of the Boutros laboratory for helpful discussions. This work was supported in part by the Deutsche Forschungsgemeinschaft (SFB873 “Stem Cells in Development and Disease”). The authors declare no competing financial interests.

Appendix A. Supplementary data

Supplementary data to this article can be found online at http://dx.doi.org/10.1016/j.scr.2016.10.010.

References

Augustin, I., Goidts, V., Bongers, A., Kerr, G., Vollert, G., Radlwimmer, B., Hartmann, C., Herold-Mende, C., Reifenberger, G., von Deimling, A., et al., 2012. The Wnt secretion protein Evi/Gpr177 promotes glioma tumourigenesis. EMBO Mol. Med. 4, 38–51.

Augustin, I., Gross, J., Baumann, D., Korn, C., Kerr, G., Grigoryan, T., Mauch, C., Birchmeier, W., Boutros, M., 2013. Loss of epidermal Evi/Wls results in a phenotype resembling psoriasiform dermatitis. J. Exp. Med. 210, 1761–1777.

Bakre, M.M., Hoi, A., Mong, J.C., Koh, Y.Y., Wong, K.Y., Stanton, L.W., 2007. Generation of multipotential mesendodermal progenitors from mouse embryonic stem cells via sustained Wnt pathway activation. J. Biol. Chem. 282, 31703–31712.

Banziger, C., Soldini, D., Schutt, C., Zipperlen, P., Hausmann, G., Basler, K., 2006. Wntless, a conserved membrane protein dedicated to the secretion of Wnt proteins from signaling cells. Cell 125, 509–522.

Bartscherer, K., Boutros, M., 2008. Regulation of Wnt protein secretion and its role in gradient formation. EMBO Rep. 9, 977–982.

Bartscherer, K., Pelte, N., Ingelfinger, D., Boutros, M., 2006. Secretion of Wnt ligands requires Evi, a conserved transmembrane protein. Cell 125, 523–533.

Becht, E., Goc, J., Germain, C., Giraldo, N.A., Dieu-Nosjean, M.C., Sautes-Fridman, C., Fridman, W.H., 2014. Shaping of an effective immune microenvironment to and by cancer cells. Cancer Immunol. Immunother. 63, 991–997.

Blatner, N.R., Mulcahy, M.F., Dennis, K.L., Scholtens, D., Bentrem, D.J., Phillips, J.D., Ham, S., Sandall, B.P., Khan, M.W., Mahvi, D.M., et al., 2012. Expression of RORgammat marks a pathogenic regulatory T cell subset in human colon cancer. Sci. Transl. Med. 4, 164ra159.

Dai, W., Liu, F., Li, C., Lu, Y., Lu, X., Du, S., Chen, Y., Weng, D., Chen, J., 2016. Blockade of Wnt/beta-catenin pathway aggravated silica-induced lung inflammation through Tregs regulation on Th immune responses. Mediat. Inflamm. 2016, 6235614.

de Visser, K.E., Eichten, A., Coussens, L.M., 2006. Paradoxical roles of the immune system during cancer development. Nat. Rev. Cancer 6, 24–37.

Ding, Y., Shen, S., Lino, A.C., Curotto de Lafaille, M.A., Lafaille, J.J., 2008. Beta-catenin stabilization extends regulatory T cell survival and induces anergy in nonregulatory T cells. Nat. Med. 14, 162–169.

Dressel, R., 2011. Effects of histocompatibility and host immune responses on the tumorigenicity of pluripotent stem cells. Semin. Immunopathol. 33, 573–591.

Dressel, R., Schindehutte, J., Kuhlmann, T., Elsner, L., Novota, P., Baier, P.C., Schillert, A., Bickeboller, H., Herrmann, T., Trenkwalder, C., et al., 2008. The tumorigenicity of mouse embryonic stem cells and in vitro differentiated neuronal cells is controlled by the recipients' immune response. PLoS One 3, e2622.

Driessens, G., Zheng, Y., Gajewski, T.F., 2010. Beta-catenin does not regulate memory T cell phenotype. Nat. Med. 16, 513–514 (author reply 514-515).

Dunn, G.P., Bruce, A.T., Ikeda, H., Old, L.J., Schreiber, R.D., 2002. Cancer immunoediting: from immunosurveillance to tumor escape. Nat. Immunol. 3, 991–998.

Dunn, G.P., Old, L.J., Schreiber, R.D., 2004. The immunobiology of cancer immunosurveillance and immunoediting. Immunity 21, 137–148.

Fridman, W.H., Dieu-Nosjean, M.C., Pages, F., Cremer, I., Damotte, D., Sautes-Fridman, C., Galon, J., 2013. The immune microenvironment of human tumors: general significance and clinical impact. Cancer Microenviron. 6, 117–122.

Fu, J., Jiang, M., Mirando, A.J., Yu, H.M., Hsu, W., 2009. Reciprocal regulation of Wnt and Gpr177/mouse Wntless is required for embryonic axis formation. Proc. Natl. Acad. Sci. U. S. A. 106, 18598–18603.

Gattinoni, L., Zhong, X.S., Palmer, D.C., Ji, Y., Hinrichs, C.S., Yu, Z., Wrzesinski, C., Boni, A., Cassard, L., Garvin, L.M., et al., 2009. Wnt signaling arrests effector T cell differentiation and generates CD8+ memory stem cells. Nat. Med. 15, 808–813.

Gooden, M.J., de Bock, G.H., Leffers, N., Daemen, T., Nijman, H.W., 2011. The prognostic influence of tumour-infiltrating lymphocytes in cancer: a systematic review with meta-analysis. Br. J. Cancer 105, 93–103.

Grumolato, L., Liu, G., Haremaki, T., Mungamuri, S.K., Mong, P., Akiri, G., Lopez-Bergami, P., Arita, A., Anouar, Y., Mlodzik, M., et al., 2013. Beta-catenin-independent activation of TCF1/LEF1 in human hematopoietic tumor cells through interaction with ATF2 transcription factors. PLoS Genet. 9, e1003603.

Hadrup, S., Donia, M., Thor Straten, P., 2013. Effector CD4 and CD8 T cells and their role in the tumor microenvironment. Cancer Microenviron. 6, 123–133.

Hanahan, D., Weinberg, R.A., 2011. Hallmarks of cancer: the next generation. Cell 144, 646–674.

Hwang, W.T., Adams, S.F., Tahirovic, E., Hagemann, I.S., Coukos, G., 2012. Prognostic significance of tumor-infiltrating T cells in ovarian cancer: a meta-analysis. Gynecol. Oncol. 124, 192–198.

Jin, J., Morse, M., Frey, C., Petko, J., Levenson, R., 2010. Expression of GPR177 (Wntless/Evi/sprinter), a highly conserved Wnt-transport protein, in rat tissues, zebrafish embryos, and cultured human cells. Dev. Dyn. 239, 2426–2434.

Jin, X., Lin, T., Xu, Y., 2015. Stem cell therapy and immunological rejection in animal models. Curr. Mol. Pharmacol.

Keerthivasan, S., Aghajani, K., Dose, M., Molinero, L., Khan, M.W., Venkateswaran, V., Weber, C., Emmanuel, A.O., Sun, T., Bentrem, D.J., et al., 2014. Beta-catenin promotes colitis and colon cancer through imprinting of proinflammatory properties in T cells. Sci. Transl. Med. 6, 225ra228.

Lee, A.S., Tang, C., Rao, M.S., Weissman, I.L., Wu, J.C., 2013. Tumorigenicity as a clinical hurdle for pluripotent stem cell therapies. Nat. Med. 19, 998–1004.

Iida, T., Iwahashi, M., Katsuda, M., Ishida, K., Nakamori, M., Nakamura, M., Naka, T., Ojima, T., Ueda, K., Hayata, K., Nakamura, Y., Yamaue, H., 2011. Tumor-infiltrating CD4 +Th17 cells produce IL-17 in tumor microenvironment and promote tumor progression in human gastric cancer. Oncol. Rep. 25 (5), 1271–1277.

Lin, S., Talbot, P., 2011. Methods for culturing mouse and human embryonic stem cells. Methods Mol. Biol. 690, 31–56.

Liu, X., Yu, X., Zack, D.J., Zhu, H., Qian, J., 2008. TiGER: a database for tissue-specific gene expression and regulation. BMC Bioinform. 9, 271.

Liu, T., Wang, Y., Peng, X., Zhang, L., Cheng, J., Jin, H., Wu, M., Qian, Q., 2012. Establishment of mouse teratocarcinomas stem cells line and screening genes responsible for malignancy. PLoS One 7, e43955.

Lu, D., Li, Y., Liu, Q.R., Wu, Q., Zhang, H., Xie, P., Wang, Q., 2015. Wls promotes the proliferation of breast cancer cells via Wnt signaling. Med. Oncol. 32, 140.

Ma, J., Wang, R., Fang, X., Ding, Y., Sun, Z., 2011. Critical role of TCF-1 in repression of the IL-17 gene. PLoS One 6, e24768.

Martin, F., Apetoh, L., Ghiringhelli, F., 2012. Controversies on the role of Th17 in cancer: a TGF-β-dependent immunosuppressive activity? Trends Mol. Med. Dec;18, 742–749.

Mi, H., Lazareva-Ulitsky, B., Loo, R., Kejariwal, A., Vandergriff, J., Rabkin, S., Guo, N., Muruganujan, A., Doremieux, O., Campbell, M.J., et al., 2005. The PANTHER database of protein families, subfamilies, functions and pathways. Nucleic Acids Res. 33, D284–D288.

Mittal, D., Gubin, M.M., Schreiber, R.D., Smyth, M.J., 2014. New insights into cancer immunoediting and its three component phases–elimination, equilibrium and escape. Curr. Opin. Immunol. 27, 16–25.

Muranski, P., Borman, Z.A., Kerkar, S.P., Klebanoff, C.A., Ji, Y., Sanchez-Perez, L., Sukumar, M., Reger, R.N., Yu, Z., Kern, S.J., et al., 2011. Th17 cells are long lived and retain a stem cell-like molecular signature. Immunity 35, 972–985.

Nakano, O., Sato, M., Naito, Y., Suzuki, K., Orikasa, S., Aizawa, M., Suzuki, Y., Shintaku, I., Nagura, H., Ohtani, H., 2001. Proliferative activity of intratumoral CD8(+) T-lymphocytes as a prognostic factor in human renal cell carcinoma: clinicopathologic demonstration of antitumor immunity. Cancer Res. 61, 5132–5136.

Nelson, B.H., 2010. CD20+ B cells: the other tumor-infiltrating lymphocytes. J. Immunol. 185, 4977–4982.

Notani, D., Gottimukkala, K.P., Jayani, R.S., Limaye, A.S., Damle, M.V., Mehta, S., Purbey, P.K., Joseph, J., Galande, S., 2010. Global regulator SATB1 recruits beta-catenin and regulates T(H)2 differentiation in Wnt-dependent manner. PLoS Biol. 8, e1000296.

Port, F., Basler, K., 2010. Wnt trafficking: new insights into Wnt maturation, secretion and spreading. Traffic 11, 1265–1271.

Posfai, E., Tam, O.H., Rossant, J., 2014. Mechanisms of pluripotency in vivo and in vitro. Curr. Top. Dev. Biol. 107, 1–37.

Prlic, M., Bevan, M.J., 2011. Cutting edge: beta-catenin is dispensable for T cell effector differentiation, memory formation, and recall responses. J. Immunol. 187, 1542–1546.

Przyborski, S.A., 2005. Differentiation of human embryonic stem cells after transplantation in immune-deficient mice. Stem Cells 23, 1242–1250.

Sato, E., Olson, S.H., Ahn, J., Bundy, B., Nishikawa, H., Qian, F., Jungbluth, A.A., Frosina, D., Gnjatic, S., Ambrosone, C., et al., 2005. Intraepithelial CD8+ tumor-infiltrating lymphocytes and a high CD8+/regulatory T cell ratio are associated with favorable prognosis in ovarian cancer. Proc. Natl. Acad. Sci. U. S. A. 102, 18538–18543.

Schreiber, R.D., Old, L.J., Smyth, M.J., 2011. Cancer immunoediting: integrating immunity's roles in cancer suppression and promotion. Science 331, 1565–1570.

Sharma, P., Shen, Y., Wen, S., Yamada, S., Jungbluth, A.A., Gnjatic, S., Bajorin, D.F., Reuter, V.E., Herr, H., Old, L.J., et al., 2007. CD8 tumor-infiltrating lymphocytes are predictive of survival in muscle-invasive urothelial carcinoma. Proc. Natl. Acad. Sci. U. S. A. 104, 3967–3972.

Song, W.K., Park, K.M., Kim, H.J., Lee, J.H., Choi, J., Chong, S.Y., Shim, S.H., Del Priore, L.V., Lanza, R., 2015. Treatment of macular degeneration using embryonic stem cell-derived retinal pigment epithelium: preliminary results in Asian patients. Stem Cell Rep. 4, 860–872.

Spranger, S., Bao, R., Gajewski, T.F., 2015. Melanoma-intrinsic beta-catenin signalling prevents anti-tumour immunity. Nature 523, 231–235.

Sprowl, S., Waterman, M.L., 2013. Past visits present: TCF/LEFs partner with ATFs for beta-catenin-independent activity. PLoS Genet. 9, e1003745.

Tang, C., Drukker, M., 2011. Potential barriers to therapeutics utilizing pluripotent cell derivatives: intrinsic immunogenicity of in vitro maintained and matured populations. Semin. Immunopathol. 33, 563–572.

van Loosdregt, J., Fleskens, V., Tiemessen, M.M., Mokry, M., van Boxtel, R., Meerding, J., Pals, C.E., Kurek, D., Baert, M.R., Delemarre, E.M., et al., 2013. Canonical Wnt signaling negatively modulates regulatory T cell function. Immunity 39, 298–310.

Voloshanenko, O., Erdmann, G., Dubash, T.D., Augustin, I., Metzig, M., Moffa, G., Hundsrucker, C., Kerr, G., Sandmann, T., Anchang, B., et al., 2013. Wnt secretion is required to maintain high levels of Wnt activity in colon cancer cells. Nat. Commun. 4, 2610.

Wang, L., Yi, T., Kortylewski, M., Pardoll, D.M., Zeng, D., Yu, H., 2009. IL-17 can promote tumor growth through an IL-6-Stat3 signaling pathway. J. Exp. Med. 206 (7), 1457–1464.

Weisel, K.C., Kopp, H.G., Moore, M.A., Studer, L., Barberi, T., 2010. Wnt1 overexpression leads to enforced cardiomyogenesis and inhibition of hematopoiesis in murine embryonic stem cells. Stem Cells Dev. 19, 745–751.

Wettenhall, J.M., Smyth, G.K., 2004. limmaGUI: a graphical user interface for linear modeling of microarray data. Bioinformatics 20, 3705–3706.

Yaguchi, T., Goto, Y., Kido, K., Mochimaru, H., Sakurai, T., Tsukamoto, N., Kudo-Saito, C., Fujita, T., Sumimoto, H., Kawakami, Y., 2012. Immune suppression and resistance mediated by constitutive activation of Wnt/beta-catenin signaling in human melanoma cells. J. Immunol. 189, 2110–2117.

Yu, Q., Sharma, A., Sen, J.M., 2010. TCF1 and beta-catenin regulate T cell development and function. Immunol. Res. 47, 45–55.

Zhao, D.M., Yu, S., Zhou, X., Haring, J.S., Held, W., Badovinac, V.P., Harty, J.T., Xue, H.H., 2010. Constitutive activation of Wnt signaling favors generation of memory CD8 T cells. J. Immunol. 184, 1191–1199.

Zhao, T., Zhang, Z.N., Rong, Z., Xu, Y., 2011. Immunogenicity of induced pluripotent stem cells. Nature 474, 212–215.

Zirakzadeh, A.A., Marits, P., Sherif, A., Winqvist, O., 2013. Multiplex B cell characterization in blood, lymph nodes, and tumors from patients with malignancies. J. Immunol. 190, 5847–5855.